


ARTICLE

Open Access

Modulation of alternative splicing induced by paclitaxel in human lung cancer

Ziran Zhu¹, Dan Chen², Wenjing Zhang¹, Jinyao Zhao¹, Lili Zhi¹, Fang Huang¹, Haoyu Ji¹, Jinrui Zhang¹, Han Liu¹, Lijuan Zou¹ and Yang Wang¹ 

Abstract

Paclitaxel is utilized as the first-line chemotherapeutic regimen for the majority of advanced non-small-cell lung carcinoma. However, whether paclitaxel could suppress cancer progression through modulating RNA alternative splicing remains largely unknown. Here, we demonstrated the effects of paclitaxel on cell proliferation inhibition, cell cycle arrest, and apoptosis. Mechanistically, paclitaxel leads to transcriptional alteration of networks involved in DNA replication and repair, chromosome segregation, chromatin silencing at rDNA, and mitosis at the transcriptional level. Moreover, paclitaxel regulates a number of cancer-associated RNA alternative splicing events, including genes involved in cellular response to DNA damage stimulus, preassembly of GPI anchor in ER membrane, transcription, and DNA repair. In particular, paclitaxel modulates the splicing of ECT2, a key factor involved in the regulation of cytokinesis. Briefly, paclitaxel favors the production of ECT2-S, the short splicing isoforms of ECT2, thereby inhibiting cancer cell proliferation. Our study provides mechanistic insights of paclitaxel on RNA alternative splicing regulation, thus to offer a potential novel route for paclitaxel to inhibit cancer progression.

Introduction

Lung cancer is one of the most common malignant cancers world-wide. In 2017, 222,500 new cancer cases and 155,870 deaths were estimated in lung and bronchus according to the American Cancer Society, in which, non-small-cell lung carcinoma (NSCLC) accounts for 83% of lung cancer¹. Most patients with stage III and IV NSCLC receive chemotherapy with or without radiation. Paclitaxel, a microtubule inhibitor, is commonly used in advanced NSCLC treatment either in combination with platinum-based agents or as monotherapy². It is well established that Paclitaxel functions by directly binding to polymerized β -tubulin, thereby resulting in perturbation

of microtubules dynamics³. Paclitaxel inhibits the dynamic instability of the mitotic spindle, leading to impaired chromosome alignment⁴. Consequently, cells are arrested by the spindle checkpoint at the G2/M phase and eventually go through apoptosis⁵. Multiple cellular pathways participate in paclitaxel-induced cytotoxicity, including RAS, MYC-controlled pathway, and inhibition of spleen tyrosine kinase^{6–8}. However, further molecular mechanisms about paclitaxel might need to be discovered due to the clinical complexity.

Almost 95% of genes are alternatively spliced in humans. Importantly, alternative splicing (AS) of pre-messenger RNA (mRNA) leads to the production of multiple mature mRNAs and protein isoforms with distinct structural and functional properties⁹. Dysregulation of AS also leads to aberrant protein isoforms, which may contribute to tumor initiation, progression, and therapeutic treatments difficulties^{10, 11}. Previously, in NSCLC, some pre-mRNA splicing regulators have been demonstrated to be abnormally expressed, including SRSF1, SRSF2, SRPK1, and SRPK2¹². In addition, Shultz et al.¹³

Correspondence: Lijuan Zou (lijuanzou1963@163.com) or Yang Wang (yangwang@dmu.edu.cn)

¹Institute of Cancer Stem Cell & Radiotherapy Oncology Department of the Second Affiliated Hospital, Dalian Medical University, Dalian 116044, China

²Department of Pathology, the First Affiliated Hospital, Dalian Medical University, Dalian 116011, China

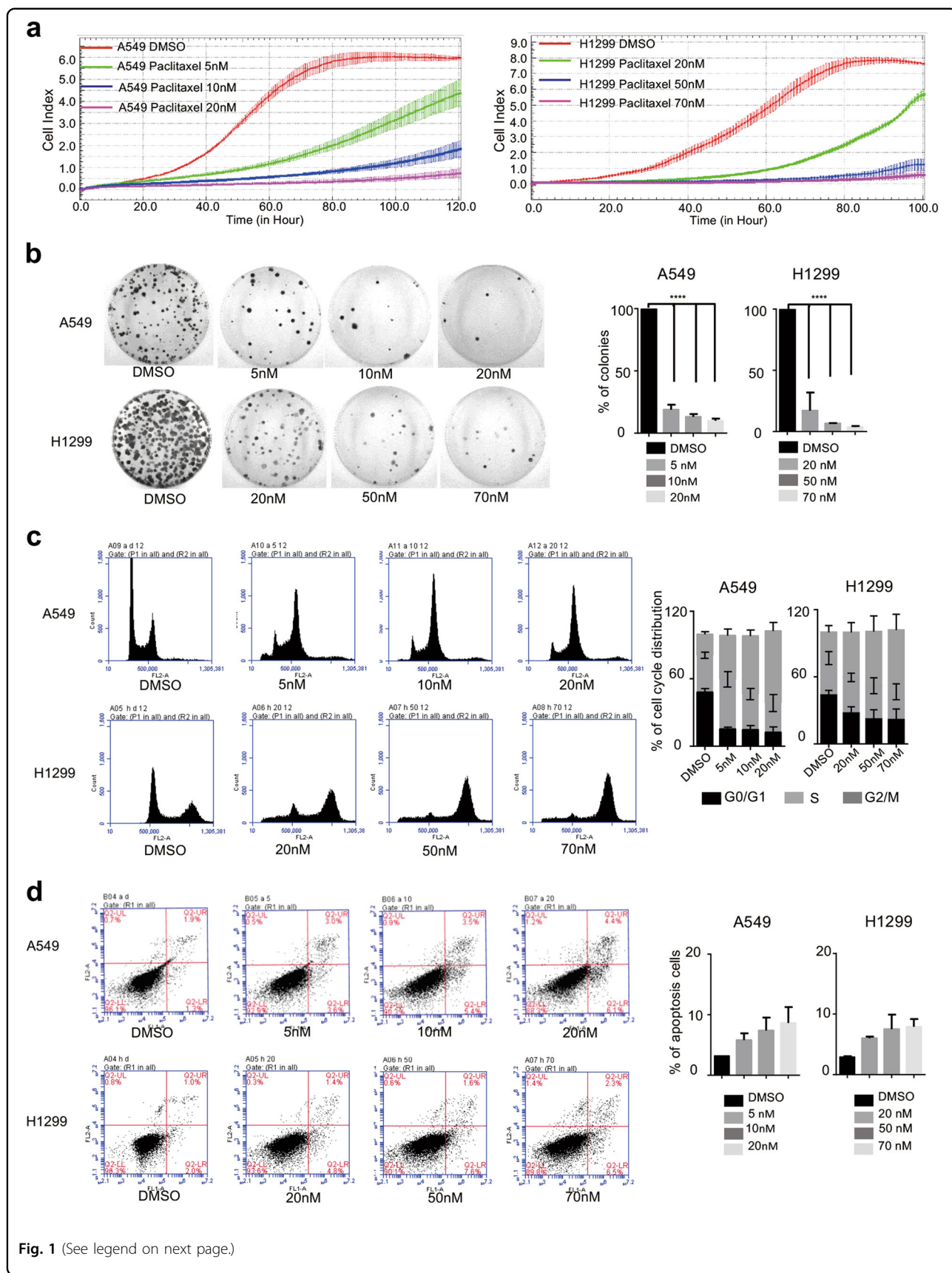
These authors contributed equally: Ziran Zhu, Dan Chen, Wenjing Zhang, Jinyao Zhao.

Edited by A. Stephanou

© The Author(s) 2018



Open Access This article is licensed under a Creative Commons Attribution 4.0 International License, which permits use, sharing, adaptation, distribution and reproduction in any medium or format, as long as you give appropriate credit to the original author(s) and the source, provide a link to the Creative Commons license, and indicate if changes were made. The images or other third party material in this article are included in the article's Creative Commons license, unless indicated otherwise in a credit line to the material. If material is not included in the article's Creative Commons license and your intended use is not permitted by statutory regulation or exceeds the permitted use, you will need to obtain permission directly from the copyright holder. To view a copy of this license, visit <http://creativecommons.org/licenses/by/4.0/>.



(see figure on previous page)

Fig. 1 Paclitaxel inhibits cell proliferation and induces cell cycle arrest and apoptosis. **a** Growth curve assays were conducted to evaluate the effects of paclitaxel on the proliferation of the non-small-cell lung carcinoma cell lines A549 and H1299. **b** Colony formation assays were performed in A549 and H1299 cells treated for 24 h with different concentrations of paclitaxel. Representative pictures of the whole plates are shown. Three experiments were carried out with corresponding data normalized to control and expressed as mean \pm SD (***)indicated $p < 0.001$. **c** Flow cytometry approach was utilized to analyze the cell cycle and apoptosis **d** of cells treated with different dosages of paclitaxel (5, 10, 20 nM for A549 cells) and (20, 50, 70 nM for H1299 cells) for 12 h respectively. *indicated $p < 0.05$

employed RNA oligonucleotides to modulate caspase 9 pre-mRNA splicing in favor of caspase 9b production, resulting in an increase in the IC₅₀ of non-small-cell lung cancer cells to paclitaxel. Moreover, in paclitaxel resistant triple-negative breast cancer cells, aberrant RNA splicing was defined, and the interaction of TRA2A with the splicing factor hnRNP M can co-regulate AS¹⁴. Taken together, these data suggest that as a chemotherapeutic agent, paclitaxel may suppress cancer cell proliferation by modulating the AS of cancer-related genes. However, the mechanistic details underlying such splicing regulation upon paclitaxel treatment are still largely unknown.

Here, we report that paclitaxel can function as a chemotherapeutic drug by modulating cancer-related splicing events in lung cancer cells. To systematically identify the splicing events regulated by paclitaxel, we performed RNA-Seq on paclitaxel treated or control lung cancer cells. Interestingly, in addition to gene expression changes, we discovered that extensive AS occurred upon paclitaxel treatment. Briefly, we identified 994 significantly differentially expressed genes, and 855 AS events after paclitaxel treatment in A549 cells. Our results suggested that paclitaxel predominantly induced skipped exons compared to other splicing types. We identified distinct AS events of FMNL3, ZMIZ2, ECT2, PLD2, and DDIT3, which may be involved in cancer cell proliferation, epithelia-mesenchymal transition and actin cytoskeleton organization. Most importantly, lung cancer cells expressing ECT2-S appeared to be more sensitive to paclitaxel. Taken together, our results not only identified mRNAs regulated by paclitaxel in NSCLC, but also suggest that AS switch might provide an alternative new route for paclitaxel to suppress cancer progression.

Results

Paclitaxel inhibits cell proliferation and induces cell cycle arrest and apoptosis

We sought to investigate the effect of paclitaxel on lung cancer cells. To this end, cell viability was determined by MTT assay after 48 h treatment with different concentrations of paclitaxel and the IC₅₀ of A549 and H1299 cells were 7.22 nM and 40.78 nM, respectively

(Supplementary Fig. 1a). Importantly, paclitaxel exhibits potent cell cytotoxicity in a dose-dependent manner, as demonstrated in two lung cancer cell lines, including A549 and H1299. Briefly, A549 cells were incubated with paclitaxel for 24 h at different concentrations (5, 10, 20 nM), whereas H1299 cells were treated with paclitaxel at 20, 50, 70 nM for 24 h. Subsequently, cells were collected to analyze the cell proliferation and growth as judged by real-time cell analyzer (RTCA) and colony formation assay (Fig. 1a, b). The treatment with 5 nM of paclitaxel showed an obvious inhibition of cell growth and higher concentrations (10 and 20 nM) showed much stronger inhibition. Similar phenotypes were also obtained from H1299 cells (Fig. 1a, b). In addition, cell migration was suppressed after paclitaxel treatment (Supplementary Fig. 1b). Moreover, when treated with distinct concentrations of paclitaxel, A549 and H1299 cells demonstrated a dose-dependent cell cycle arrest at G2/M phase, as well as a decreased G1 phase, as judged by FACS (Fig. 1c). We also measured the apoptosis, and found that about 10% apoptotic population was achieved at the maximum concentration of paclitaxel treatment in A549 and H1299 cells, respectively (Fig. 1d). Taken together, we demonstrated that paclitaxel potently induced cell growth inhibition, G2/M cell cycle arrest, and apoptosis in lung cancer cells.

Systematic identification of gene expression changes induced by paclitaxel

To further investigate the molecular mechanisms of paclitaxel-induced cell growth inhibition, we performed high-throughput mRNA sequencing (mRNA-seq) with A549 cells treated by paclitaxel at 7.22 nM for 72 h. Strikingly, we identified 994 genes with significant expression change (twofold with adjusted $p < 0.05$). Subsequent gene ontology analysis showed that DNA replication, mitotic nuclear division, DNA damage, chromosome segregation, and G2/M transition of mitotic cell cycle were the most enriched pathways (Fig. 2a). In addition, most of paclitaxel-induced genes were functionally associated with networks that contains genes involved in cell cycle regulation, DNA damage response and DNA replication, as judged by the Search Tool for the Retrieval of Interacting Genes/Proteins (STRING)

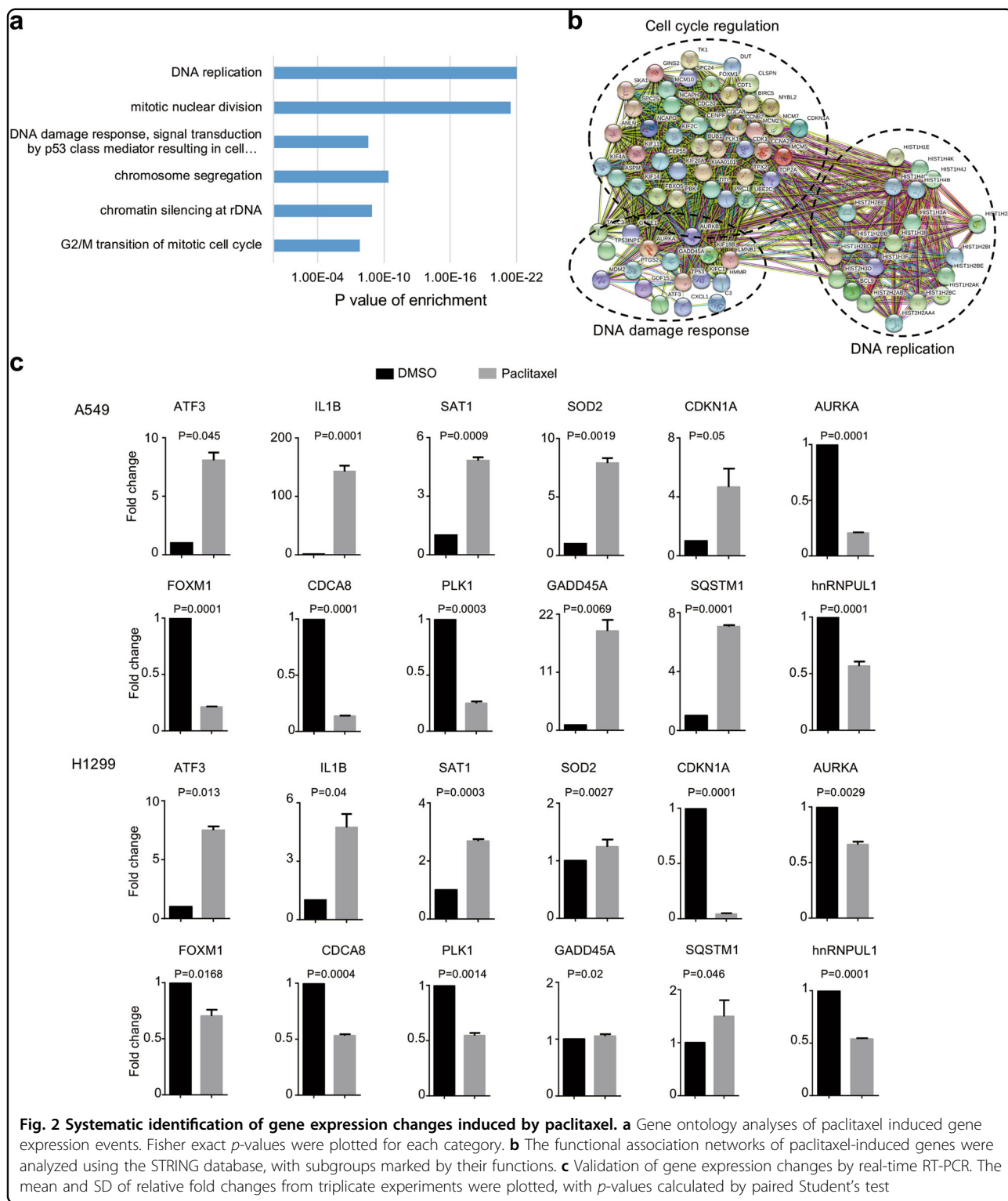
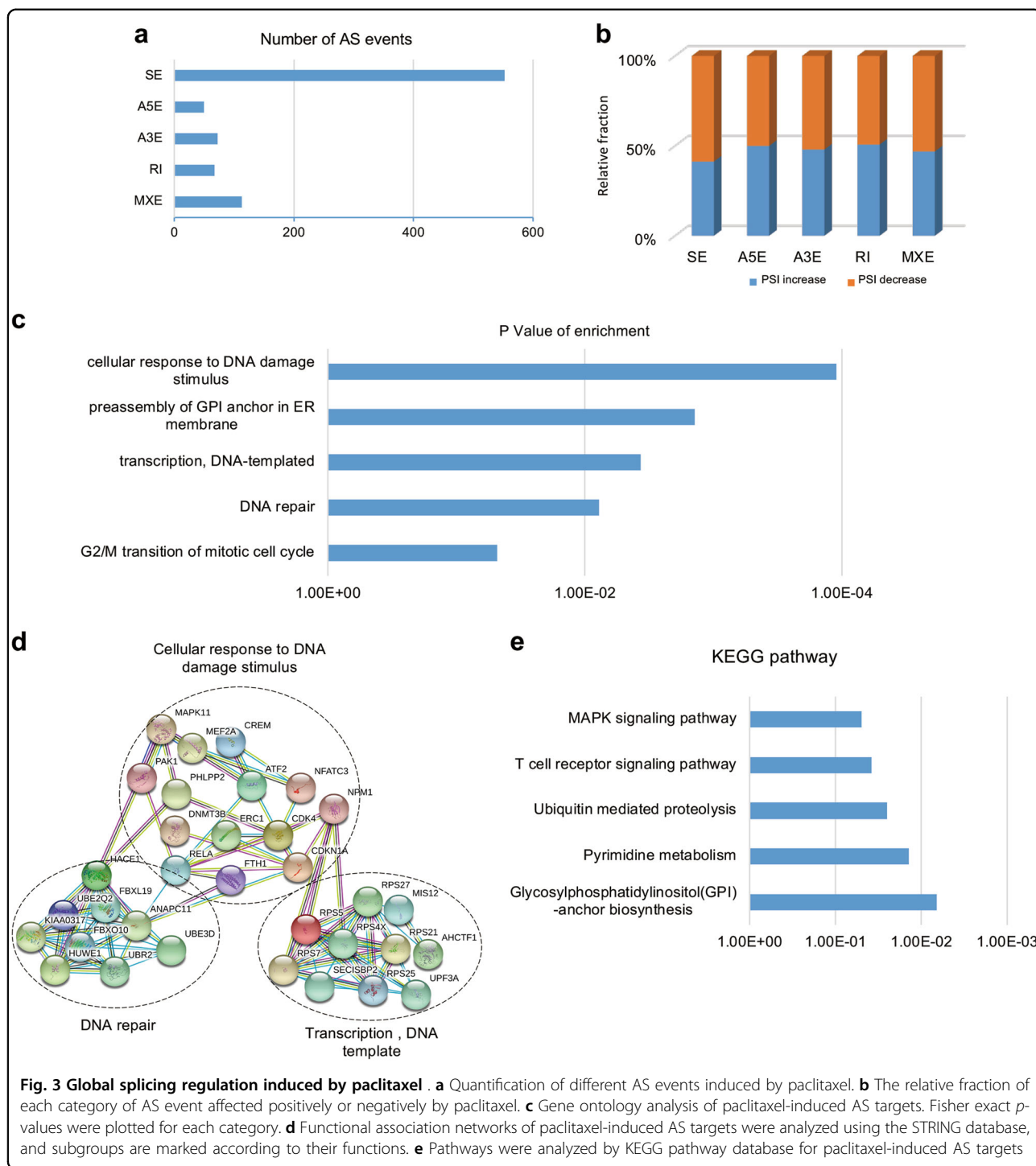


(Fig. 2b). We further randomly validated several targets induced by paclitaxel with real-time reverse transcription (RT)-PCR (Fig. 2c). Among these genes, GADD45A, AURKA are involved in DNA damage and regulation of

apoptotic process. CDKN1A, AURKA, FOXM1, and PLK1 are involved in the regulation of cell cycle. Interestingly, some of the splicing factors were also affected by paclitaxel, such as hnRNPUL1 for example, indicating that



paclitaxel might also inhibit cancer cell growth through modulating RNA AS.

Global regulation of AS induced by paclitaxel in cancer-related genes

To explore the effects of paclitaxel on alteration of AS, we systematically analyzed the mRNA-seq data to identify

differentially changed AS events. As expected, we obtained 855 paclitaxel-regulated AS events with an obvious change of percent-spliced-in (PSI) values (the change of PSI > 0.15), including 552 skipped exons (SE), 50 alternative 5' ss exon (A5E), 73 alternative 3' ss (A3E), 67 retained intron (RI), and 113 mutually exclusive exons (MXE) (Fig. 3a). Subsequent analysis indicated that the

majority of AS events were negatively regulated in cells treated with paclitaxel (Fig. 3b).

Using gene ontology (GO) analysis, the paclitaxel-induced splicing events were enriched in groups related to cell response to DNA damage stimulus, preassembly of GPI anchor in ER membrane, DNA-templated transcription, DNA repair and G2/M transition of mitotic cell cycle (Fig. 3c). These targets are consistent with the diversity of global gene expression induced by paclitaxel. In addition, we conducted STRING analysis and found that many of the paclitaxel-induced splicing targets were functionally connected into well-linked interaction networks, including genes involved in DNA damage, DNA repair, and DNA template-dependent transcription (Fig. 3d). Meanwhile, we performed KEGG analysis and found that interactions induced by paclitaxel were focused on MAPK signaling pathway, T-cell receptor signaling pathway and GPI-anchor biosynthesis (Fig. 3e). Collectively, these results suggested that the biological processes affected by paclitaxel are related to DNA damage, DNA repair, and cell cycle, which is consistent with functions of paclitaxel on microtubules.

Alternative splicing switch induced by paclitaxel

We subsequently validated the splicing switch of six randomly chosen targets from the mRNA-seq results. As expected, we demonstrated that exon 4 skipping of ECT2 (GEF epithelial cell transforming sequence 2) was significantly induced by paclitaxel. Similarly, the skipping of exon 8 of ZMIZ2 (zinc finger MIZ-type containing 2) and exon 6 of FMNL3 (formin-like 3) were also elevated after paclitaxel treatment (Fig. 4a and Supplementary Fig. 2). Meanwhile, we further verified that paclitaxel promoted the upstream 3' ss usage of ELF2 (ETS transcription factor 2) and DDIT3 (DNA damage inducible transcript 3) (Fig. 4b and Supplementary Fig. 2), whereas paclitaxel inhibited the distal 5' ss usage of PLD2 (phospholipase D2) (Fig. 4c). Among these genes, ECT2 regulates cytokinesis in non-transformed cells by acting RhoA^{15, 16}. ECT2 is over-expressed in multiple cancers^{17–19}. It is reported that ECT2 depletion impairs tumorigenic growth of NSCLC cell²⁰. ZMIZ2 plays a role in regulating the activity of the Wnt/ β -catenin signaling pathway²¹. FMNL3 is involved in regulation of cell morphology and cytoskeletal organization²². Thus, we next sought to investigate whether the splicing switch of ECT2 is indeed involved in the paclitaxel-mediated cancer inhibition.

ECT2 splicing switch participated in paclitaxel-induced lung cancer inhibition

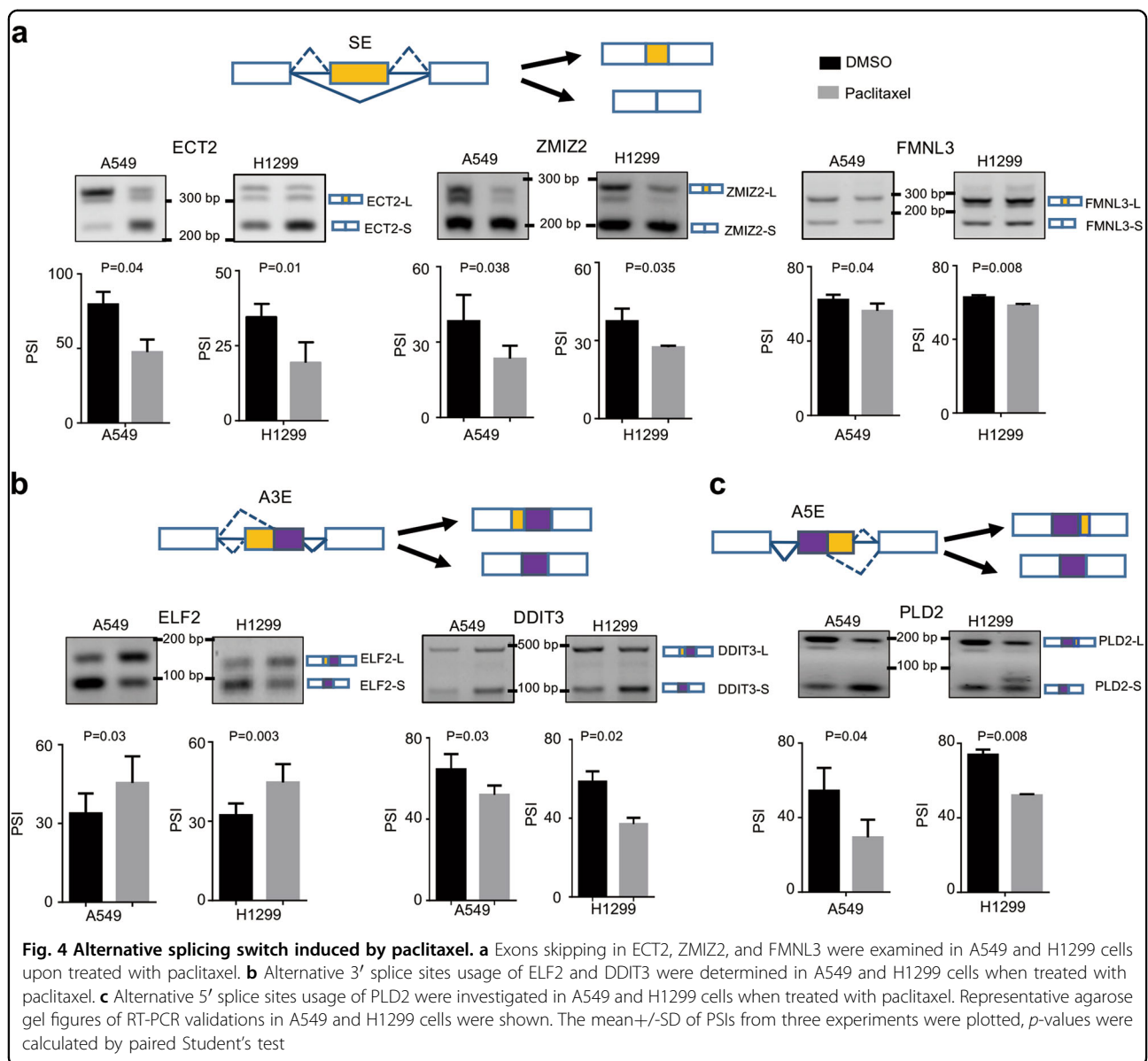
We have demonstrated that paclitaxel induced the skipping of exon 4 of ECT2, which resulted in a frame shift in the BRCT domain of ECT2 (Fig. 4a). Importantly,

ECT2 was reported to promote nucleotide exchange on Rho family members of small GTPase, known to regulate ribosomal RNA (rRNA) synthesis through a PKC-Ect-Rac1-NPM signaling axis that is required for lung tumorigenesis. Therefore, we aimed to determine the role of the short isoform of ECT2-S in cancer progression, especially in paclitaxel-mediated cancer suppression. To this end, we stably expressed two isoforms of ECT2, ECT2-L, or ECT2-S, in A549 and H1299 cells (Supplementary Fig. 3a, b). We treated cells with paclitaxel and found that ECT2-L was predominantly nucleus-localized, whereas ECT2-S was distributed in both cytoplasm and nucleus as examined by immunofluorescence (Supplementary Fig. 3c). Strikingly, we found cells expressing ECT2-S grew evidently slower than control and ECT2-L expressing cells as judged by RTCA and colony formation assays (Fig. 5a, b). These data suggested that ECT2-S, the short isoform, could inhibit cancer cell proliferation, which has the opposite function to the canonical full-length ECT2.

Subsequently, we investigated whether ECT2-S can suppress cancer cell growth synergistically with paclitaxel. To this end, we treated cells stably expressing ECT2-L or ECT2-S with paclitaxel for 24 h respectively. We further applied the resulting cells to examine the cell viability by using the CCK8 and colony formation assays. As expected, A549 cells stably expressing ECT2-S could significantly inhibit cancer cell growth as compared to control cells, whereas cells expressing ECT2-L could promote cancer cell growth compared to control cells (Fig. 5c, d). Consistently, such results were also confirmed in another lung cancer cell line, H1299 (Fig. 5c, d). To further validate the synergistic effect of ECT2-S with paclitaxel, we treated cells stably expressing ECT2-S or ECT2-L with different concentrations of paclitaxel and examined the cell viability. The data demonstrated that the combined treatment of ECT2-S with paclitaxel could markedly inhibit cancer cell proliferation in both A549 and H1299 cells (Fig. 5e). Collectively, ECT2 splicing switch participated in paclitaxel-induced lung cancer inhibition.

ECT2-S is reduced in cancer samples and negatively correlated to survival

To further determine the clinical significance of ECT2 splicing in patients, we tested the relative levels of two ECT2 isoforms in paired lung cancer samples and the adjacent normal tissues surgically obtained from six patients. As compared to the paired normal samples, the relative mRNA levels of ECT2-S were significantly reduced in five out of six tested primary NSCLC specimens (Fig. 6a, b), suggesting a common reduction of ECT2-S expression despite obvious heterogeneity in different tumor samples. Consistent with our results,



analyses of RNA-seq datasets from the TCGA consortium demonstrated that ECT2-S levels were markedly decreased in lung adenocarcinoma, lung squamous carcinoma, and head and neck cancer (Fig. 6c).

Additionally, we also analyzed the expression level of ECT2-L in various large scale studies from TCGA, and found ECT2-L is evidently elevated in multiple cancers, including lung, breast, colon, renal, esophageal, liver cancer, and so on (Fig. 6d and Supplementary Fig. 4a–d).

Intriguingly, we applied Kaplan–Meier Plotter to analyze the overall survival of cancer patients with distinct ECT2-L levels using datasets from large scale screening. As expected, higher expression of ECT2-L was related to poor overall survival in patients with lung, breast, ovarian, and gastric cancer (Fig. 6e and

Supplementary Fig. 4e). These data further proved that paclitaxel might suppress cancer progression through mediating ECT2 splicing.

Discussion

Paclitaxel remains the first-line standard therapy regimen with platinum agent or singly in the second-line setting for advanced and metastatic NSCLC. Paclitaxel suppresses tumorigenesis primarily through interfering with mitotic spindle dynamics and triggering the mitotic checkpoint, thereby inducing an extended G2/M arrest. Thus, such cycle arrest can lead to cell death via the mitochondrial apoptotic pathway. Aberrant AS exerts control over major hallmarks of cancer, including apoptosis, epithelial-mesenchymal transition, and tumor

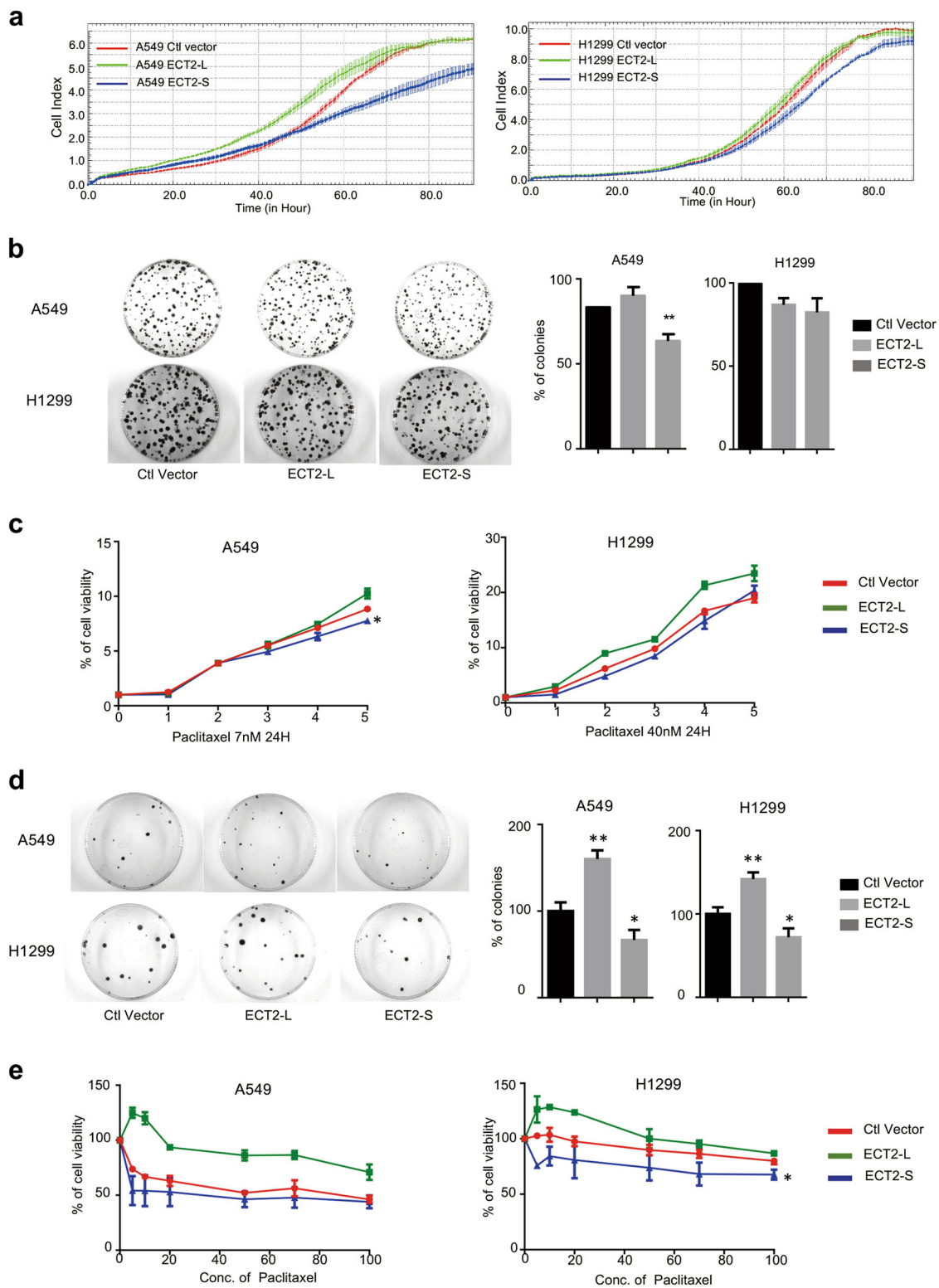
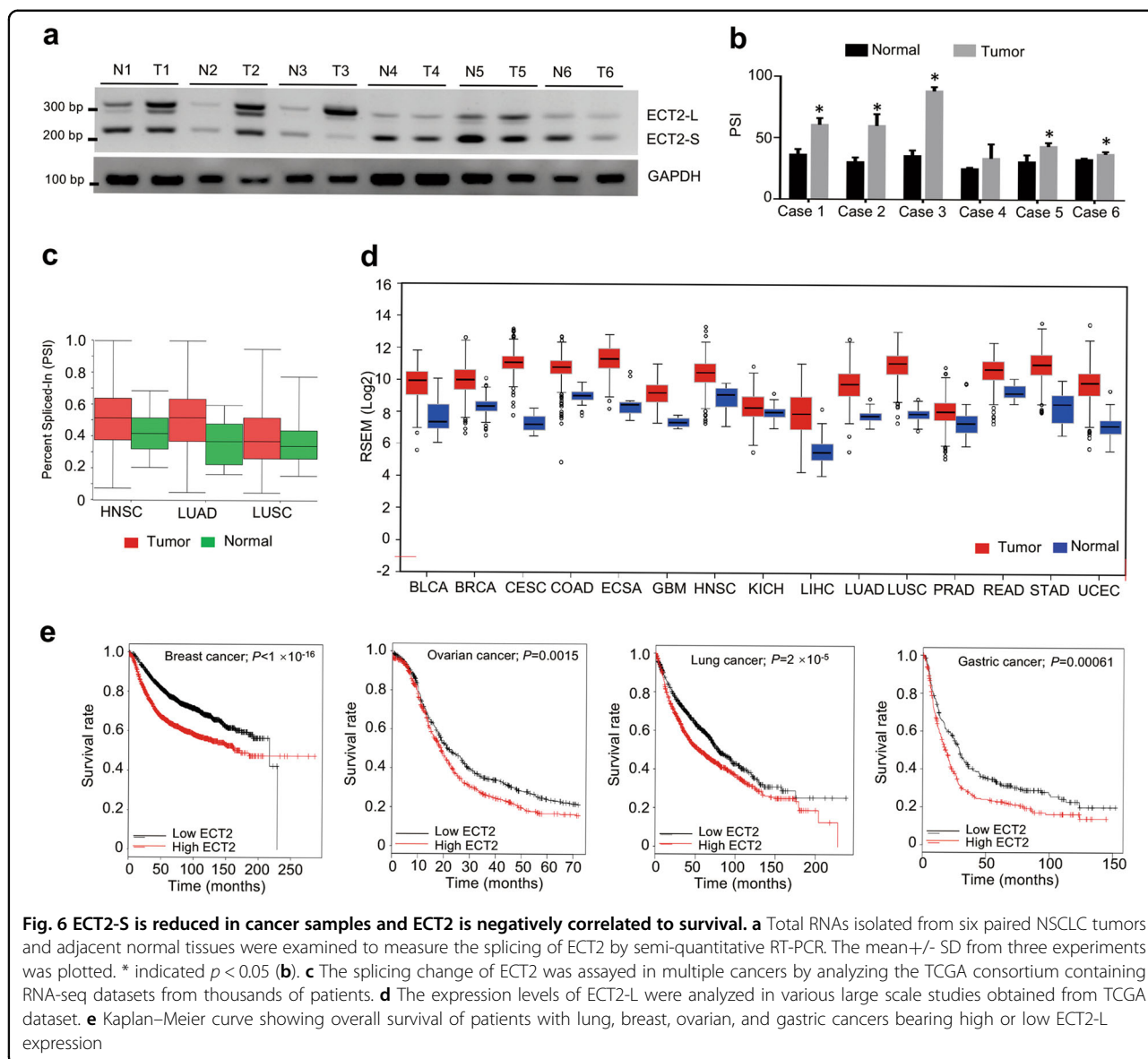


Fig. 5 ECT2 splicing switch participated in paclitaxel-induced lung cancer inhibition. **a** Cell proliferation of A549 and H1299 cells stably expressing ECT2-L or ECT2-S were analyzed using RTCA assay. **b** The growth of A549 and H1299 cells stably expressing ECT2-L or ECT2-S were analyzed by colony formation assay. **c** A549 and H1299 cells stably expressing ECT2-L or ECT2-S were incubated with 7.22 nM or 40 nM paclitaxel for 24 h, respectively, and then the cell viability and growth were analyzed by CCK8 and colony formation assays (**d**). The mean \pm SD of relative colony numbers were plotted, with *p*-values calculated by Student's test. **e** A549 and H1299 cells stably expressing ECT2-L or ECT2-S were treated with different concentrations of paclitaxel, and the cell viability was examined by CCK8 assay



proliferation and invasion. Moreover, numerous splicing variants of specific genes serve as molecular markers of cancer or directly mediate cancer pathogenesis^{23–26}. Accumulating evidence suggests that different alternatively spliced transcripts were involved in response to clinical therapeutic drugs. In our model, we demonstrated that paclitaxel could inhibit cancer progression through regulating the AS of many cancer-related genes. Specifically, paclitaxel could switch the splicing of ECT2 from the canonical full-length isoform towards the short isoform ECT2-S, which in turn inhibit cancer cell proliferation. That is because normally the phosphorylation of ECT2 will activate Rho family GTPase to promote cancer progression. However, the skipping of exon 4 results in a disruption of the BRCT domain of ECT2,

which offers a binding pocket for phosphorylated residues. Thus, the short isoform of ECT2 inhibits tumorigenesis specifically when treated with paclitaxel. Importantly, ECT2 has been shown to be involved in Wingless/Wnt signaling pathway, and controlling cleavage furrow formation during cytokinesis^{27, 28}. Therefore, our results represent a novel mechanism for paclitaxel to suppress cancer progression through modulating AS of cancer-related genes.

In addition to ECT2 splicing, other splicing events might also contribute the suppression of tumorigenesis upon paclitaxel treatment. Using RNA-seq analysis, we also found that paclitaxel mediated some splicing events for several genes associated with DNA damage, transcription, DNA repair, and G2/M transition of mitotic cell

cycle. For instance, paclitaxel controls splicing of FMNL3 and PLD2, which play critical roles in the regulation of cytoskeletal organization. These data suggest that paclitaxel regulates many splicing events critical to tumorigenesis, which might provide new therapeutic combinations to sensitize cancer cells to paclitaxel treatment.

Materials and Methods

Cell culture and treatment

Human lung cancer A549 and NCI-H1299 cell lines were obtained from the American Type Culture Collection (Manassas, VA, USA). Paclitaxel (S1150) was purchased from Selleck.cn. These cells were maintained in F12K Kaighn's Modification and RPMI-1640 supplemented with 10% Fetal Bovine Serum (FBS) respectively. To stably overexpress ECT2-L/S in A549 and H1299 cells, we used lentiviral vectors. We transfected 293t cells with pCDH-3 × Flag-ECT2-L/S or pCDH-3 × Flag empty vectors according to the manufacturer's protocols. We collected the supernatant media containing virus by centrifugation to remove any cellular contaminant. Further, A549 and H1299 cells were infected with the viral particles, and the stably integrated cells were selected with 5 µg/ml puromycin for 5 days. Then cells were maintained in medium containing 2 µg/ml puromycin. All cells were maintained at 37 °C in a humidified incubator with 5% CO₂. The expression of transgenes was confirmed by western blots and RT-PCR before further analysis.

Cell cycle and apoptosis analysis by flow cytometry

Cells were seeded in 60 mm-dish (160,000 cells/per dish) and allowed to grow overnight for 70% confluency. To analyze the cell cycle regulation induced by paclitaxel, A549 or H1299 cells were treated with paclitaxel, at the final concentration of 5, 10, 20 nM and 20, 50, 70 nM, respectively for 12 h. Cells were harvested and washed by PBS and then fixed with 75% cold ethanol overnight. Before analyzed by flow cytometry, we incubated the cells with RNase in 37 °C water for 30 min, stained with propidium iodide for 30 min on ice and in dark. Different cell populations were quantified based on DNA contents to discern cells with 2N (G1), S-phase, and 4N (G2/M), and fragment DNA (apoptotic cells). To illustrate apoptosis effects by paclitaxel, cells were treated for 24 h, then dissociated from culture plates using trypsin without EDTA. Cells were washed with PBS for two times and re-suspended in binding buffer and stained with Annexin V and propidium iodide prior to analysis using flow cytometry.

RT-PCR and quantitative RT-PCR validation

We extracted total RNA from cells treated with or without paclitaxel using Trizol reagent (Invitrogen) according to the manufacturer's instructions. Genome

DNAs were removed by 30 min DNase I (Takara) treatment at 37 °C and then heat inactivation using 50 nM EDTA. Total RNA (2 µg) was then reverse-transcribed with PrimeScript RT reagent kit (Takara) with random primer, and 1 µl of the cDNA was used as the template for PCR amplification. RT-PCR products were separated on 3% gels. The amount of each splicing isoform was measured by comparison of the integrated optical density of detected bands using the GIS 1D Gel Image System (ver. 4.2; Tanon). The primers used for gene expression are shown in table. Real-time quantitative PCR was performed using Takara SYBR II kit on system according to the manufacturer's instructions.

Western blot

Cells were harvested with RIPA lysis buffer containing 1 mM Na₃VO₄, 1 mM Cocktail and 1 mM PMSF. Cell debris was removed by centrifugation. The protein samples (20 µg) were boiled of 5 min in 1 × SDS sample buffer and fractionated by 10% sodium dodecyl sulfate polyacrylamide gel electrophoresis and transferred to nitrocellulose membrane. The following antibodies were used: Flag (Sigma), TUBULIN (T5168). Bound antibodies were visualized with the ECL kit (ncmbio).

RNA-sequencing analysis

A549 cells were treated with paclitaxel 7.22 nM or DMSO for 72 h, and then total RNAs were extracted using Trizol. We used the Illumina TruSeq Total RNA Sample Prep kits to purify poly-adenylated RNA (not exceeding 2 µg) after RNase free DNase digested as per manufactures instruction. Cytoplasmic rRNA was removed by the RiboZero Human. Prior to generation of cDNA library with bar coded ends the mRNA purified were further analyzed using Bio-analyzer (Agilent Technologies). The protocol employed to prepare RNA-seq libraries was based on the use of Illumina TruSeq Total RNA Sample Prep kits. The cluster generation and sequencing were carried out by standard procedures in HiSeq 2000 Illumina platform with pair-end 150 bp (PE 150) sequencing strategy.

The paired-end sequences were mapped to human genome (hg38) using MapSplice 2.0.1.6 (default parameters) to discover splicing junctions. Further analyzed the mapped reads with Cufflinks can calculate the level of gene expression. We analyzed the changes of splicing isoforms using MISO package with annotation of all known AS events, and the results filtered according to the percent-spliced in values.

We performed gene ontology analysis using DAVID GO analysis software to search for enriched pathways. The functional association of Paclitaxel-induced targets were resolved using protein interaction data from STRING database, and we investigated the generating functional

interaction networks. The sub-network containing more than five nodes were demonstrated.

The RNA-seq dataset was deposited to the Gene Expression Omnibus with accession number

Cytotoxicity assay and inhibitory concentration 50 measurement

Cell growth determination kit (MTT) was used to detect the IC₅₀. Briefly, cells were separately seeded into 96-well plates (4000 cells/well) to culture overnight and then treated with paclitaxel at different concentrations (0, 5, 10, 20, 50, 70, 100 nM) in 100 μ l culture medium. After 48 h culture, 10 μ l MTT solution was added and incubated for 4 h at 37 °C. Spectrophotometrically measure absorbance at a wavelength of 570 nm was performed. Dose–response curves were plotted to determine half maximal IC₅₀ of paclitaxel using the Graphpad Prism6.

Colony formation assay

A549 and H1299 cells or stable expression ECT2-L/S cells treated without or with stepwise concentrations of paclitaxel 24 h were seeded in 60-mm dishes (300 cells per dish) and incubated at 37 °C, 5% CO₂ in humidified incubator for 2 weeks (updated with fresh medium every 4 days). Each treatment was carried out in triplicate. Colonies were fixed with 4% paraformaldehyde and stained with crystal violet solution. Numbers of colonies was counted.

Immunofluorescence staining

A549 and H1299 cells stably expression pCDH-ECT2-L/S were cultured on sterile glass cover slips, treated with 7.22 nM and 40 nM paclitaxel 12 h at 37 °C. Cells were washed briefly with PBS and then fixed 10 min with methanol. Blocking with 3% BSA in PBS for 20 min after PBS washing. Rinse sections in PBS-Tween 20 for 10 min. PBS wash and then incubated with primary antibody (Flag antibody) overnight at 4 °C. Incubated with anti-Mouse secondary antibody. Counterstain with DAPI and then captured images with a fluorescent microscope.

Real-time cell analysis by RTCA

The RTCA instrument was used to assess the cell viability, proliferation, and migration of A549, H1299, and stably expression ECT2-L/S cells or cells treated with different concentration of Paclitaxel for 24 h. Cells were digested with trypsin briefly, counted and then re-suspended in culture medium. Background measurements were taken from the wells by adding 50 μ l of the same medium to the E-16 plates. Subsequently, cells were plated at a density of 2000/well with fresh medium to a final volume of 150 μ l. Cells were incubated for 30 min at room temperature and then analyzed in the RTCA in 5% CO₂ and 37 °C incubator. The impedance signals were recorded every 5 min until the end of the experiment (up to 100 h). The migration assay

was also tested by using cell invasion and migration plates (CIM-plates). Cell index for real-time dynamic assessment and slope calculations for the migration assessments were calculated automatically by the RTCA Software Package 1.2 of the RTCA system.

Statistical analysis

Differences between experimental groups were evaluated by one-way ANOVA or Student test using Graphpad Prism 6 software package to analyze colony formation, cell cycle, apoptosis, and splicing changes. Statistical significance was based on a *p*-value of 0.05.

Acknowledgements

We thank members of the Wang laboratory for their technical support and discussions throughout the study. This work was supported by the National Natural Science Foundation of China (81422038, 91540110, and 31471235 to Y. W.; 31400726 to W. Z.); Young Thousand Talents Program of China (to Y.W.); the Department of Science and Technology of Dalian City (the “Dalian Supports High Level Talents Innovation and Entrepreneurship Program” 2016RJ02 to Y. W.); the Education Department of Liaoning Province in China (the “Program for Pan-Deng Scholars” to Y.W.); the Newton Advanced Fellowship from the Academy of Medical Sciences in UK (JXR11831 to Y.W.).

Author details

¹Institute of Cancer Stem Cell & Radiotherapy Oncology Department of the Second Affiliated Hospital, Dalian Medical University, Dalian 116044, China.

²Department of Pathology, the First Affiliated Hospital, Dalian Medical University, Dalian 116011, China

Conflict of interest

The authors declare that they have no conflict of interest.

Publisher's note

Springer Nature remains neutral with regard to jurisdictional claims in published maps and institutional affiliations.

Supplementary Information accompanies this paper at <https://doi.org/10.1038/s41419-018-0539-4>.

Received: 22 January 2018 Revised: 25 March 2018 Accepted: 27 March 2018

Published online: 30 April 2018

References

- Siegel, R. L., Miller, K. D. & Jemal, A. Cancer Statistics, 2017. *CA Cancer J. Clin.* **67**, 7–30 (2017).
- Langer, C. J. et al. Randomized, phase III trial of first-line figitumumab in combination with paclitaxel and carboplatin versus paclitaxel and carboplatin alone in patients with advanced non-small-cell lung cancer. *J. Clin. Oncol.* **32**, 2059–2066 (2014).
- Schmidt, M. & Bastians, H. Mitotic drug targets and the development of novel anti-mitotic anticancer drugs. *Drug Resist. Updat.* **10**, 162–181 (2007).
- Zasadil, L. M. et al. Cytotoxicity of paclitaxel in breast cancer is due to chromosome missegregation on multipolar spindles. *Sci. Transl. Med.* **6**, 229ra243 (2014).
- Torres, K. & Horwitz, S. B. Mechanisms of Taxol-induced cell death are concentration dependent. *Cancer Res.* **58**, 3620–3626 (1998).
- Yang, L. et al. Mutations of p53 and KRAS activate NF- κ B to promote chemoresistance and tumorigenesis via dysregulation of cell cycle and suppression of apoptosis in lung cancer cells. *Cancer Lett.* **357**, 520–526 (2015).
- Topham, C. et al. MYC is a major determinant of mitotic cell fate. *Cancer Cell* **28**, 129–140 (2015).

8. Yu, Y. et al. Inhibition of spleen tyrosine kinase potentiates paclitaxel-induced cytotoxicity in ovarian cancer cells by stabilizing microtubules. *Cancer Cell* **28**, 82–96 (2015).
9. Matlin, A. J., Clark, F. & Smith, C. W. Understanding alternative splicing: towards a cellular code. *Nat. Rev. Mol. Cell Biol.* **6**, 386–398 (2005).
10. David, C. J. & Manley, J. L. Alternative pre-mRNA splicing regulation in cancer: pathways and programs unhinged. *Genes Dev.* **24**, 2343–2364 (2010).
11. Oltean, S. & Bates, D. O. Hallmarks of alternative splicing in cancer. *Oncogene* **33**, 5311–5318 (2014).
12. Gout, S. et al. Abnormal expression of the pre-mRNA splicing regulators SRSF1, SRSF2, SRPK1 and SRPK2 in non small cell lung carcinoma. *PLoS ONE* **7**, e46539 (2012).
13. Shultz, J. C. et al. SRSF1 regulates the alternative splicing of caspase 9 via a novel intronic splicing enhancer affecting the chemotherapeutic sensitivity of non-small cell lung cancer cells. *Mol. Cancer Res.* **9**, 889–900 (2011).
14. Liu, T. et al. TRA2A promoted paclitaxel resistance and tumor progression in triple-negative breast cancers via regulating alternative splicing. *Mol. Cancer Ther.* **16**, 1377–1388 (2017).
15. Saito, S. et al. Rho exchange factor ECT2 is induced by growth factors and regulates cytokinesis through the N-terminal cell cycle regulator-related domains. *J. Cell. Biochem.* **90**, 819–836 (2003).
16. Matthews, H. K. et al. Changes in Ect2 localization couple actomyosin-dependent cell shape changes to mitotic progression. *Dev. Cell* **23**, 371–383 (2012).
17. Chen, J. et al. ECT2 regulates the Rho/ERK signalling axis to promote early recurrence in human hepatocellular carcinoma. *J. Hepatol.* **62**, 1287–1295 (2015).
18. Justilien, V. et al. Ect2-dependent rRNA synthesis is required for KRAS-TRP53-driven lung adenocarcinoma. *Cancer Cell* **31**, 256–269 (2017).
19. Kanada, M., Nagasaki, A. & Uyeda, T. Q. Stabilization of anaphase midzone microtubules is regulated by Rho during cytokinesis in human fibrosarcoma cells. *Exp. Cell Res.* **315**, 2705–2714 (2009).
20. Baker, M. J., Cooke, M. & Kazanietz, M. G. Nuclear PKC α -ECT2-Rac1 and ribosome biogenesis: A novel axis in lung tumorigenesis. *Cancer Cell* **31**, 167–169 (2017).
21. Lee, S. H. et al. Identification of a novel role of ZMIZ2 protein in regulating the activity of the Wnt/ β -catenin signaling pathway. *J. Biol. Chem.* **288**, 35913–35924 (2013).
22. Thompson, M. E., Heimsath, E. G., Gauvin, T. J., Higgs, H. N. & Kull, F. J. FMNL3 FH2-actin structure gives insight into formin-mediated actin nucleation and elongation. *Nat. Struct. Mol. Biol.* **20**, 111–118 (2013).
23. Lukas, J. et al. Alternative and aberrant messenger RNA splicing of the mdm2 oncogene in invasive breast cancer. *Cancer Res.* **61**, 3212–3219 (2001).
24. Venables, J. P. Unbalanced alternative splicing and its significance in cancer. *Bioessays* **28**, 378–386 (2006).
25. Safikhani, Z. et al. Gene isoforms as expression-based biomarkers predictive of drug response in vitro. *Nat. Commun.* **8**, 1126 (2017).
26. Yi, P. et al. Bcl-rambo beta, a special splicing variant with an insertion of an Alu-like cassette, promotes etoposide- and Taxol-induced cell death. *FEBS Lett.* **534**, 61–68 (2003).
27. Hara, T. et al. Cytokinesis regulator ECT2 changes its conformation through phosphorylation at Thr-341 in G2/M phase. *Oncogene* **25**, 566–578 (2006).
28. Reiter, L. T., Seagroves, T. N., Bowers, M. & Bier, E. Expression of the Rho-GEF Pbl/ECT2 is regulated by the UBE3A E3 ubiquitin ligase. *Hum. Mol. Genet.* **15**, 2825–2835 (2006).